1 Thermodynamic functions

1.1 INTRODUCTION

Thermodynamics facilitates the linking together of "the many observable properties so that they can be seen to be a consequence of a few" [1]. It provides a firm basis for the rules that macroscopic systems follow at equilibrium. When combined with phenomena associated with the approach to equilibrium, it forms the foundations of kinetic theory. It was on this basis that Zener attempted to rationalise the transformations that occur in steels [2, 3] so that the effect of alloying elements, atomic mobility, nucleation and mechanism could all be incorporated into a single hypothesis.

After an introduction to some essential concepts, the remainder of this chapter deals with theory that is relevant particularly to iron and its solutions.

1.2 DEFINITIONS

1.2.1 INTERNAL ENERGY AND ENTHALPY

The change in the internal energy ΔU of a closed system can be written as

$$\Delta U = q - w \tag{1.1}$$

where q is the heat transferred into the system and w, the work done by the system. The sign convention is that heat added and work done by the system are positive, whereas heat given off and work done on the system are negative. Equation 1.1 may be written in differential form as

$$\mathrm{d}U = \mathrm{d}q - \mathrm{d}w. \tag{1.2}$$

For the special case where the system does work against a constant atmospheric pressure, this becomes

$$\mathrm{d}U = \mathrm{d}q - P\mathrm{d}V \tag{1.3}$$

where P is the pressure and V the volume.

The specific heat capacity of a material represents its ability to absorb or emit heat during a unit change in temperature. Heat changes the distribution of energy amongst the particles in the system (atoms, electrons, ...) and it is these fundamental mechanisms that control the heat capacity, defined formally as $\mathrm{d}q/\mathrm{d}T$. Since $\mathrm{d}q = \mathrm{d}U + P\mathrm{d}V$, the specific heat capacity measured at constant volume is given by:

$$C_{\mathrm{V}} = \left(\frac{\partial U}{\partial T}\right)_V.$$

It is convenient to define a new function H, the enthalpy of the system:

$$H = U + PV.$$

A change in enthalpy accounts for both the heat absorbed at constant pressure, and the work done by the $P\Delta V$ term. The specific heat capacity measured at constant pressure is therefore given by:

$$C_{\mathrm{P}} = \left(\frac{\partial H}{\partial T}\right)_P.$$

Heat capacity can be measured using a variety of calorimetric methods. The data can then be used to estimate enthalpy changes as a function of temperature and pressure:

$$\Delta H = \int_{T_1}^{T_2} C_P \, dT. \tag{1.4}$$

1.2.2 ENTROPY, FREE ENERGY

In the reversible Carnot cycle, a gas is placed in contact with a heat reservoir at temperature T_2, expands isothermally on absorbing a quantity of heat q_2, in the process doing work $-w_1$. The gas is then insulated and expands adiabatically, does work $-w_2$ as its temperature drops to T_1. It is then placed in contact with a heat reservoir at T_1, compressed reversibly and isothermally with work w_3 done upon it and giving up heat $-q_1$ to the reservoir. To complete the cycle, the gas is insulated, compressed reversibly and adiabatically by doing work w_4 upon it, causing its temperature to rise back to T_2 [4]. The change in internal energy $\Delta U = q_1 + q_2 + w$ on completion of the cycle is therefore zero, where $w = \Sigma_{i=1}^{4} w_i$. The work output of the engine, $-w$, is the difference between heat taken and heat returned to the reservoirs, i.e. $-w = q_2 - (-q_1)$ so the maximum efficiency is defined as the ratio of the work output to the heat absorbed:

$$\text{efficiency} = \frac{-w}{q_2} = \frac{q_2 + q_1}{q_2}.$$

Kelvin used this to define the absolute temperature,

$$\text{efficiency} = \frac{q_2 + q_1}{q_2} = \frac{T_2 - T_1}{T_2} \quad \text{so that} \quad \frac{q_2}{T_2} + \frac{q_1}{T_1} = 0. \tag{1.5}$$

By considering a cyclic process in terms of infinitesimal parts [4], it can be demonstrated that the following relationship holds for any reversible cycle,

$$\frac{\mathrm{d}q_2}{T_2} + \frac{\mathrm{d}q_1}{T_1} = 0 \quad \text{with} \quad \oint \frac{\mathrm{d}q}{T} = 0$$

making the quantity $\mathrm{d}q/T$ a function of state S with

$$\mathrm{d}S = \frac{\mathrm{d}q}{T} \tag{1.6}$$

Clausius during the 19th century named this function S as entropy; in the absence of any change in enthalpy, a reaction can occur spontaneously and irreversibly in an isolated system if it leads to an increase in entropy, i.e., $\Delta S > 0$. It is evident that in general, neither the enthalpy nor the entropy change can in isolation be assumed to reliably indicate the whether a reaction can occur spontaneously. The Gibbs free energy G is therefore defined as a combination of these two terms,

$$G = H - TS. \tag{1.7}$$

The Helmholtz free energy F is the corresponding term at constant volume, when H is replaced by U in Equation 1.7. A process can occur spontaneously if it leads to a reduction in the free energy. Quantities such as H, G and S are all *functions of state*.

From an experimental perspective, a change in entropy can be measured via the heat capacity:

$$\Delta S = \int_{T_1}^{T_2} \frac{C_P}{T} \, \mathrm{d}T.$$

1.2.3 CONFIGURATIONAL ENTROPY

Figure 1.1a shows a mixture of two kinds of atoms, with like atoms segregated with no mixing; there is only one way of achieving this arrangement. On the other hand, if they are allowed to mix ideally then there are many more ways of configuring them, three of which are illustrated in Figure 1.1c-d. A mixing of the atoms is obviously more *probable*.

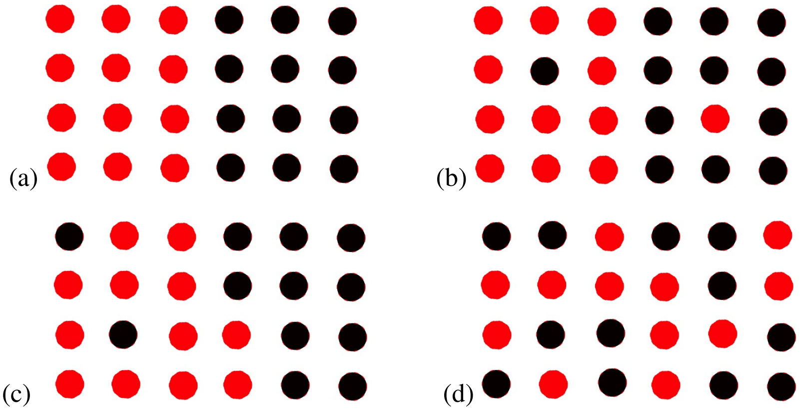

Figure 1.1 Four different configurations of a mixture of two kinds of atoms. (a) The two kinds of atoms are partitioned into their own spaces, without mixing. (b-d) If the atoms are allowed to mix then many more arrangements are possible, here only three of the many are illustrated.

Suppose there are N sites amongst which are distributed n atoms of type A and $N-n$ of type B. The first A atom can be placed in N different ways and the second in $N-1$ different ways. These two atoms cannot be distinguished so the number of different ways of placing the first two A atoms is $N(N-1)/2$. The number of distinguishable ways of placing all the atoms in this way, the number of distinguishable ways of placing all the A atoms is

$$\frac{N(N-1)\ldots(N-n+2)(N-n+1)}{n!} = \frac{N!}{n!(N-n)!}. \tag{1.8}$$

So if the atoms behave ideally, i.e., they do not have a preference for the type of neighbour, then the probability of a uniform distribution is much much more likely than the ordered distribution.

For a real system for which the number of atoms is very large, a parameter is needed that expresses the likelihood as a function of the correspondingly large number of configurations (w_c) possible. Suppose that a term S is defined such that $S \propto \ln w_c$, where the logarithm is taken because it may be necessary to add two different kinds of disorder (after Boltzmann), then the S is identified as the configurational *entropy* $S = k \ln w_c$, where k, the proportionality constant, is known as the Boltzmann constant which for a mole of atoms is the gas constant R. The entropy is a thermodynamic function of state and it is additive. When comparing scenarios, the one that is favoured on the basis of the degree of disorder is that which has the greater entropy. In terms of solutions, entropy favours mixing over separation. On this basis, it can be shown quite simply that the change in entropy when atoms mix is given by

$$\Delta S = -R\Sigma_{i=1}^{j} x_i \ln x_i$$

where $i = 1 \ldots j$ represents the atomic species and x_i its mole fraction.

1.2.4 RELATIONSHIP BETWEEN CLAUSIUS AND BOLTZMANN ENTROPIES

The Carnot engine illustrates the spreading of energy whereas the Boltzmann approach is about mixing. The relationship between these is quite straightforward – both involve mixing. As Denbigh stated with admirable elegance, “As soon as it is accepted that matter consists of small particles which are in motion it becomes evident that every large-scale natural process is essentially a process of *mixing*” [p. 110, 5]. Energy transfer involves the motion of the atoms; it was not, at the time of Carnot, known that matter consists of atoms. It really isn’t necessary to say much more.

1.3 MORE FUNCTIONS

We have seen that heat capacity data can be related directly to the thermodynamic functions of state H, G and S. Its variation with temperature and chemical composition is therefore important in determining the relative stabilities of the phases. A number of factors can contribute independently to the ability of a material to absorb energy. It has been found useful to factorise the specific heat capacities of each phase in iron, into three components with different origins.

The bulk of the contribution comes from lattice vibrations, the electrons themselves contributing in a relatively minor way because the Pauli exclusion principle prevents all of them from participating in the energy absorption process. The third contribution, which is particularly significant for iron, comes from temperature-induced magnetic changes. The net specific heat capacity at constant pressure is therefore:

$$C_{\mathrm{P}}\{T\} = C_{\mathrm{V}}^{\mathrm{L}}\left\{\frac{T_{\mathrm{D}}}{T}\right\}C_1 + C_{\mathrm{e}}T + C_{\mathrm{P}}^{\mu}\{T\}$$

where T_{D} is the Debye temperature and $C_{\mathrm{V}}^{\mathrm{L}}$ is the Debye specific heat with the function C_1 correcting $C_{\mathrm{V}}^{\mathrm{L}}$ to a specific heat at constant pressure. C_{e} is the electronic specific heat coefficient and C_{P}^{μ} the component due to magnetism.

The Debye specific heat has its origins in the vibrations of atoms, which become increasingly violent as the temperature rises [6]. These elastic waves (phonons) take discrete, quantised wavelengths consistent with being bound by the periodic lattice of atoms in the solid, although the Debye model described here is a continuum model. The atoms do not all vibrate with the same frequency, so a spectrum of vibrations is considered in deriving their contribution to the internal energy U. The maximum in the spectrum is designated the Debye frequency ω_{D}, which is proportional to the Debye temperature T_{D} at which the highest frequency mode is excited:

$$T_{\mathrm{D}} = \frac{h\omega_{\mathrm{D}}}{2\pi k}$$

where h and k are the Planck and Boltzmann constants respectively. With the approximation that the phonon frequency is proportional inversely to the wavelength, the internal energy due to the atom vibrations is:

$$U = \frac{9NkT^4}{T_{\mathrm{D}}^3}\int_0^{x_{\max}} \frac{x^3}{(e^x - 1)}\,\mathrm{d}x \tag{1.9}$$

where $x = h\omega_{\mathrm{D}}/(2\pi kT)$ and N is the total number of lattice points in the specimen. Since $C_{\mathrm{V}}^{\mathrm{L}} = \mathrm{d}U/\mathrm{d}T$, it follows that the lattice specific heat capacity at constant volume can be specified in terms of the Debye temperature and the Debye function (equation 1.9).

At low temperatures ($T \ll T_{\mathrm{D}}$), $U \rightarrow 3NkT^4\pi^4/(5T_{\mathrm{D}}^3)$ so that $C_{\mathrm{V}}^{\mathrm{L}} \rightarrow 12\pi^4NkT^3/(5T_{\mathrm{D}}^3)$ and the lattice specific heat thus follows a T^3 dependence. For $T \gg T_{\mathrm{D}}$, the lattice heat capacity can similarly be shown to become temperature independent and approach a value $3Nk$, as might be expected for N classical oscillators, each with three degrees of freedom (Figure 1.2).

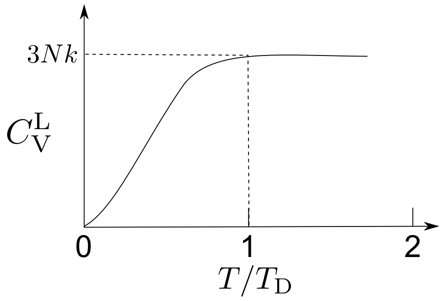

Figure 1.2 The Debye function showing how the heat capacity due to phonons varies as a function of the absolute temperature normalised by the Debye temperature.

2 Equilibrium state

2.1 CHEMICAL POTENTIAL

In a single-phase equilibrium diagram such as that for iron as a function of temperature and pressure, the boundaries between the phase fields represent the locus of all points along which the adjacent phases are in equilibrium, i.e., they have an identical free energy. For example, the α/γ phase boundary is defined by setting (Figure 2.1):

$$G^{\alpha} = G^{\gamma}. \tag{2.1}$$

This is because allotropic transitions are considered here as a function of variables such as temperature and pressure, where the crystal structure changes but not the chemical composition.

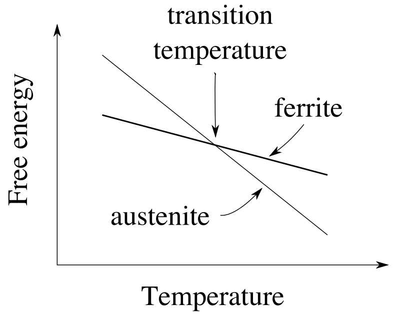

Figure 2.1 The transition temperature for an allotropic transformation.

A different approach is needed when the chemical composition is variable. Consider a single-phase alloy consisting of two components A and B. The molar free energy $G\{x\}$ of that phase will in general be a function of the mole fractions $(1-x)$ and x of A and B respectively, written as a weighted mean of the free energy contributions from each component:

$$G\{x\} = \underbrace{(1-x)\mu_{\mathrm{A}}}_{\text{contribution from A atoms}} + \underbrace{x\mu_{\mathrm{B}}}_{\text{contribution from B atoms}}. \tag{2.2}$$

The terms μ_{B} and μ_{B}, known as the *chemical potentials* per mole of A and B respectively, in effect partition the free energy $G\{x\}$ into a component purely due to A atoms and another due to B atoms alone. This equation is illustrated in Figure 2.2 by the tangent at the coordinate $[G\{x\},x]$. Consistent with Equation 2.2, the intercepts of this tangent on the vertical axes give μ_{A} and μ_{B}. Since the slope of the tangent depends on the composition, so do the chemical potentials. Note that the free energies of the pure components are written μ_{A}° and μ_{B}°.

It should be obvious from Figure 2.2 that

$$\begin{aligned} \mu_{\mathrm{A}} &= G\{x\} - x\frac{\partial G}{\partial x} \\ \text{and} \qquad \mu_{\mathrm{B}} &= G\{x\} + (1-x)\frac{\partial G}{\partial x} \end{aligned}$$

where $\partial G/\partial x$ is the slope of the tangent so the product on the right-hand side of the equations simply represents the difference in μ and G. In general, for a system with n components [97, p. 57]:

$$\mu_i = G\{x_i\} + \sum_{j=2}^{n}(\delta_{ij} - x_j)\frac{\partial G}{\partial x_j} \tag{2.3}$$

where δ_{ij} is the Kronecker delta ($\delta_{ij} = 0$ for $i \neq j$ and $\delta_{ij} = 1$ for $i = j$).

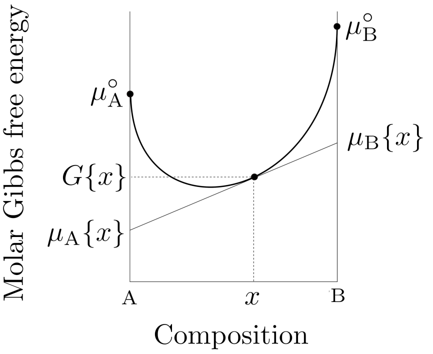

Figure 2.2 Illustration of the chemical potential μ for a binary solution, with μ° representing the free energy of the pure component.

The chemical potential $\mu\{x\}$ of a component is known also as its *partial* molar free energy, describing a part of the *integral* molar free energy $G\{x\}$. There are in fact many quantities which can be expressed using relationships of the form implied by Equation 2.2. Thus, the volume of a solution might be written in terms of the partial molar volumes of the components:

$$V_m = \overline{V}_A x_A + \overline{V}_B x_B \tag{2.4}$$

where $\overline{V}_i$ refers to the partial molar volume of component i =A,B.

2.2 EQUILIBRIUM BETWEEN SOLUTIONS

Consider now two phases α and γ that are placed in intimate contact in a binary steel. The phases will only be in equilibrium with each other if the carbon atoms in γ have the same chemical potential as the carbon atoms in α, and if this is true also for the Fe atoms:

$$\begin{aligned} \mu_C^\alpha &= \mu_C^\gamma \\ \mu_{Fe}^\alpha &= \mu_{Fe}^\gamma. \end{aligned} \tag{2.5}$$

In fact, in a binary solution, the chemical potentials of A and B when sharing a tangent are not independent so this last condition is redundant. This is apparent from Figure 2.2, where the two potentials are connected by the tangent.

If the atoms of a particular species have the same chemical potential in both the phases, then there can be no tendency for them to migrate across the phase boundaries. The system will be in stable equilibrium if this condition applies to all species of atoms. The way in which the free energy of a phase varies with concentration is unique to that phase, so the *concentration* of a particular species of atom need not be identical in phases which are at equilibrium. Therefore, in general,

$$\begin{aligned} x_C^{\alpha\gamma} &\neq x_C^{\gamma\alpha} \\ x_{Fe}^{\alpha\gamma} &\neq x_{Fe}^{\gamma\alpha} \end{aligned} \tag{2.6}$$

where $x_i^{\alpha\gamma}$ describes the mole fraction of element i in phase α which is in equilibrium with phase γ etc.

The condition that the chemical potential of each species of atom must be the same in all phases at equilibrium is general. For the binary alloy, two phase case, it follows that the equilibrium compositions can be found on a plot of free energy versus composition, by constructing a tangent that is common to the two free energy curves as illustrated in Figure 2.3.

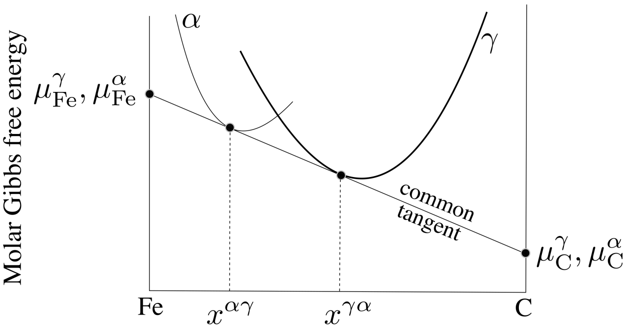

Figure 2.3 The common tangent construction giving the equilibrium compositions $x^{\alpha\gamma}$ and $x^{\gamma\alpha}$ of the two phases at a fixed temperature.

2.3 ACTIVITY

The chemical potential μ_A^α of the A atoms in the α phase may be expanded in terms of a contribution from the pure component A and a concentration dependent term as follows:

$$\mu_A^\alpha = \mu_A^{\circ\alpha} + RT \ln a_A^\alpha \tag{2.7}$$

where $\mu_A^{\circ\alpha}$ is the free energy of pure A in the structure of α, and a_A is the *activity* of atom A in the solution of A and B.

The activity of an atom in a solution can be thought of as its effective concentration in that solution. For example, there will be a greater tendency for the A atoms to evaporate from solution, when compared with pure A, if the B atoms repel the A atoms. The effective concentration of A in solution will therefore be greater than implied by its atomic fraction, i.e., its activity is greater than its concentration. The opposite would be the case if the B atoms attracted the A atoms.

The atom interactions can be expressed in terms of the change in energy as an A-A and a B-B bond is broken to create 2(A-B) bonds. An ideal solution is formed when there is no change in energy in the process of forming A-B bonds. The activity is equal to the mole fraction in an ideal solution (Figure 2.4). If, on the other hand, there is a reduction in energy than the activity is less than ideal and vice versa. The activity and concentration are related via an activity coefficient Γ:

$$a = \Gamma x. \tag{2.8}$$

The activity coefficient is in general a function of the chemical composition of all the elements present in the solution, but tends to be constant in dilute solutions (i.e., in the Henry's law region).

In this discussion, the activity of the solute was defined with respect to a Raoultian reference state, i.e., $a = 1$ for $x = 1$. Other definitions are sometimes convenient. A common alternative for dilute solutions being that the activity tends to unity as the concentration tends to 1 wt%.

Note that solutions where the enthalpy of mixing is positive tend to exhibit clustering at low temperatures whereas those with a negative enthalpy of mixing will tend to exhibit ordering at low temperatures. The effect of temperature is to mix all atoms since both clustering and ordering cause a reduction in entropy (i.e., a reduction in entropy). The product $-T\Delta S$ becomes increasingly positive at high temperatures, so much so that it eventually overcomes the enthalpy effects and causes the mixing of all atoms.

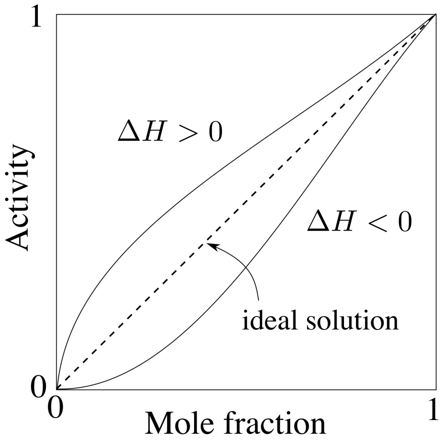

Figure 2.4 Variation in Raoultian activity as a function of its concentration in a binary solution. The ideal solution represents the case where the enthalpy of mixing is zero; the atoms are indifferent to the specific nature of their neighbours. The case where the activity is larger than the concentration is for solutions where the enthalpy of mixing is greater than zero, with like atoms preferred as near neighbours. When the activity coefficient is less than unity, unlike atoms are preferred as near neighbours, the enthalpy of mixing being negative.

2.4 IDEAL SOLUTION

An ideal solution is one in which the atoms at equilibrium are distributed randomly; the interchange of atoms within the solution causes no change in the potential energy of the system. For a binary (A-B) solution the numbers of the different kinds of bonds can therefore be calculated using simple probability theory:

$$\begin{aligned} N_{\mathrm{AA}} &= \frac{1}{2}N(1-x)^2 \\ N_{\mathrm{BB}} &= \frac{1}{2}Nx^2 \\ N_{\mathrm{AB}} &= N(1-x)x \end{aligned}$$

where N_{AB} represents both A-B and B-A bonds which cannot be distinguished. N is the total number of atoms and x the fraction of B atoms. The factor of $\frac{1}{2}$ avoids counting A-A or B-B bonds twice.

For an ideal solution, the entropy of mixing is given by Equation 3.3 with $m_{\mathrm{B}} = m_{\mathrm{A}} = 1$. There is no enthalpy of mixing since there is no change in energy when bonds between like atoms are broken to create those between unlike atoms. This is why the atoms are randomly distributed in the solution. The molar free energy of mixing is therefore:

$$\Delta G_{\mathrm{M}} = N_{\mathrm{a}}kT[(1-x)\ln\{1-x\} + x\ln\{x\}]. \tag{2.9}$$

Figure 2.5 shows how the configurational entropy and the free energy of mixing vary as a function of the concentration. ΔG_{M} is at a minimum for the equiatomic alloy because that is when the entropy of mixing is at its largest; the curves are naturally symmetrical about $x = 0.5$. The form of the curve does not change with temperature though the magnitude at any concentration scales with the temperature. It follows that at 0 K there is no difference between a mechanical mixture and an ideal solution.

From Equation 2.7, the chemical potential per mole for a component in an ideal solution is given by:

$$\mu_{\mathrm{A}} = \mu_{\mathrm{A}}^{\circ} + N_{\mathrm{a}}kT\ln\{1-x\}$$

and there is a similar equation for B. Since $\mu_{\mathrm{A}} = \mu_{\mathrm{A}}^{\circ} + RT\ln a_{\mathrm{A}}$, it follows that the activity coefficient is unity.

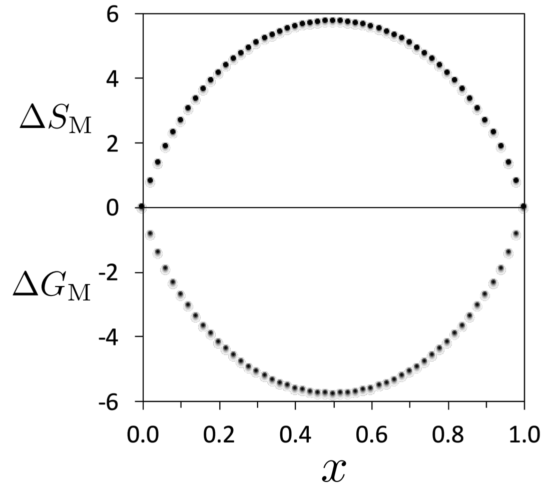

Figure 2.5 The entropy of mixing ($\mathrm{kJ\,mol^{-1}\,K^{-1}}$) and the free energy of mixing ($\mathrm{kJ\,mol^{-1}}$) as a function of concentration in an ideal binary solution where the atoms are distributed at random. The free energy is for a temperature of 1000 K. The data are plotted as dots rather than curves because concentration is strictly a discrete variable. So the slope at the vertical axes is not $\pm\infty$ as implied by Equation 2.9, but finite though very large.

2.5 REGULAR SOLUTIONS

There are no solutions of iron that are ideal. The iron-manganese liquid phase is close to ideal, though even that has an enthalpy of mixing which is about $-860\,\mathrm{J\,mol^{-1}}$ for an equiatomic solution at 1000 K, which compares with the contribution from the configurational entropy of about $-5800\,\mathrm{J\,mol^{-1}}$. The ideal solution model is nevertheless useful because it provides a reference. The free energy of mixing for a non-ideal solution often is written with an additional term, the *excess* free energy ($\Delta_e G = \Delta_e H - T\Delta_e S$) that indicates the deviation from ideality:

$$\begin{aligned}\Delta G_M &= \Delta_e G + N_a kT[(1-x)\ln\{1-x\} + x\ln\{x\}] \\ &= \Delta_e H - T\Delta_e S + N_a kT[(1-x)\ln\{1-x\} + x\ln\{x\}] \qquad (2.10)\end{aligned}$$

One of the components of the excess enthalpy of mixing comes from the change in the energy when new kinds of bonds are created during the formation of a solution. This enthalpy is, in the *regular solution* model, estimated from the pairwise interactions between adjacent atoms. The term *regular solution* was proposed by Hildebrand [98] to describe mixtures, the properties of which when plotted varied in an aesthetically regular manner; he went on to suggest that a regular solution, although not ideal, would still contain a random distribution of the constituents.[1] Following Guggenheim [99], the term regular solution is now restricted to cover mixtures that assume an ideal entropy of mixing but have a non-zero interchange energy.

In the regular solution model, the enthalpy of mixing is obtained by counting the different kinds of near neighbour bonds when the atoms are mixed at random; this information together with the binding energies gives the required change in the enthalpy on mixing. The binding energy may be defined by considering the change in energy as the distance between a pair of atoms is decreased from infinity to an equilibrium separation (Figure 2.6). The change in energy during this process is the binding energy, which for a pair of A atoms is written $-2\varepsilon_{AA}$. It follows that when $\varepsilon_{AA} + \varepsilon_{BB} < 2\varepsilon_{AB}$, the solution will have a larger than random probability of bonds between unlike atoms. The converse is true when $\varepsilon_{AA} + \varepsilon_{BB} > 2\varepsilon_{AB}$ since atoms then prefer to be neighbours to their own kind. Notice that for an ideal solution it only is necessary for $\varepsilon_{AA} + \varepsilon_{BB} = 2\varepsilon_{AB}$, and not $\varepsilon_{AA} = \varepsilon_{BB} = \varepsilon_{AB}$ [99].

Suppose now that the approximation that atoms are randomly distributed is retained, even though the enthalpy of mixing is not zero. The number of A-A, A-B and B-B bonds in a mole of solution is then $\frac{1}{2}zN_a(1-x)^2$, $\frac{1}{2}zN_a x^2$ and $zN_a(1-x)x$ respectively, where z is the co-ordination number. It

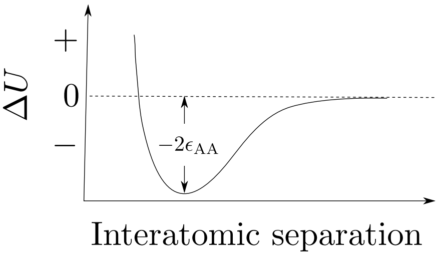

Figure 2.6 Change in energy as a function of the distance between a pair of A atoms. $-2\varepsilon_{AA}$ is the binding energy for the pair of atoms. There is a strong repulsion at close-range.

follows that the molar enthalpy of mixing is given by:

$$\Delta H_M \simeq N_a z(1-x)x\omega \qquad \text{where} \qquad \omega = \varepsilon_{AA} + \varepsilon_{BB} - 2\varepsilon_{AB}. \tag{2.11}$$

The product $zN_a\omega$ is often called the regular solution parameter, which in practice will be temperature and composition dependent. A composition dependence also leads to an asymmetry in the enthalpy of mixing as a function of composition about $x = 0.5$. For the nearly ideal Fe-Mn liquid phase solution, the regular solution parameter is $-3950 + 0.489T\,\mathrm{J\,mol^{-1}}$ if a slight composition dependence is neglected.

A positive ω favours the clustering of like atoms whereas when it is negative there is a tendency for the atoms to order. This second case is illustrated in Figure 2.7, where an ideal solution curve is presented for comparison. Like the ideal solution, the form of the curve for the case where $\Delta H_M < 0$ does not change with the temperature, but unlike the ideal solution, there is a free energy of mixing even at 0 K where the entropy term ceases to make a contribution.

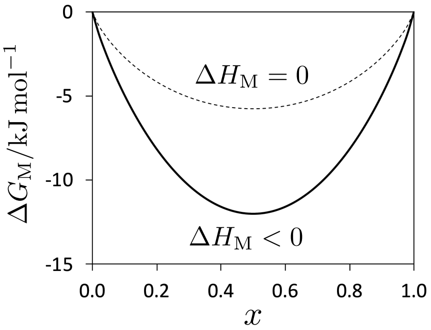

Figure 2.7 Free energy of mixing at 1000 K, as a function of concentration in a binary solution where there is a preference for unlike atoms to be near neighbours. The free energy curve for the ideal solution ($\Delta H_M = 0$) is included for reference.

The corresponding case for $\Delta H_M > 0$ is illustrated in Figure 2.8, where the form of the curve is seen to change with the temperature. The contribution from the enthalpy term can largely be neglected at high temperatures where the atoms become randomly mixed by thermal agitation so the free energy curve then has a single minimum. However, as the temperature is reduced, the opposing contribution to the free energy from the enthalpy term introduces two minima at the solute-rich and solute-poor concentrations. This is because like-neighbours are preferred. On the other hand, there is a maximum at the equiatomic composition because that gives a large number of unfavoured unlike atom bonds. Between the minima and the maximum lie points of inflexion which are of importance in spinodal decomposition, to be discussed later.

For a regular solution, Equation 2.2 shows that the chemical potential per mole is given by:

$$\mu_B = \mu_A^\circ + zN_a x^2\omega + N_a kT \ln\{1-x\} \tag{2.12}$$

and that the activity coefficient is $\exp\{zx^2\omega/kT\}$. Some of the properties of the different kinds of solutions are summarised in Table 2.1.

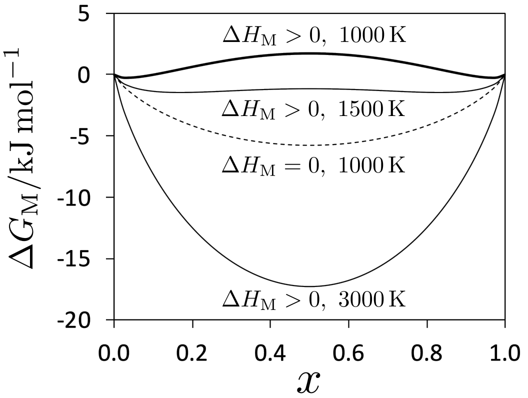

Figure 2.8 Free energy of mixing as a function of concentration and temperature in a binary solution where there is a tendency for like atoms to cluster. The free energy curve for the ideal solution ($\Delta H_{\mathrm{M}} = 0$) is included for reference.

Table 2.1
Elementary thermodynamic properties of solutions

Type	ΔS_{M}	ΔH_{M}
Ideal	Random	0
Regular	Random	$\neq 0$
Quasichemical	Not random	$\neq 0$

3 Case study: mechanical alloying

All steels are solutions. The distinction between a compound and a solution is that the free energy of the former increases sharply with a change in its chemical composition. For a solution, the variation in free energy with composition is much more gentle so that the range of composition over which it can exist is greater. It is useful to examine the nature of a solution by considering its evolution as the components are mixed together. For when is a mixture, a solution?

3.1 ALLOYING BY DEFORMATION

Mechanical alloying is a process invented by Benjamin [95], in which mixtures of fine powders consisting of elemental metals or master alloys are changed into solid solutions, apparently without any melting (Figure 3.1). The powders are forced to collide with each other and with much larger, hardened steel balls whilst contained in a ball mill. The collisions are energetic, involve large contact pressures, and lead eventually to the formation of an intimate solid solution. Refractory oxides can also be introduced into the mechanically alloyed powder for dispersion strengthening. The alloyed powder is finally extruded to form full density bulk samples in rod, sheet or other useful shapes. The process has been used commercially to make iron alloys containing large amounts of aluminium for oxidation resistance, and yttria particles to guard against creep.

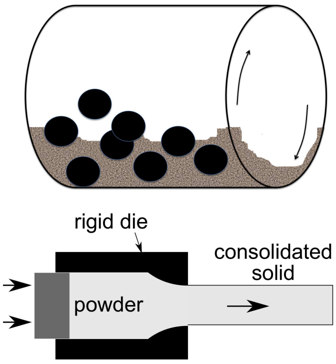

Figure 3.1 Mixture of metallic powders and compounds ball-milled together until alloying occurs. The top part shows a cylindrical drum containing a mixture of elemental powders and large steel balls. When the drum is rotated the balls collide causing the powder particles to coalesce and fragment repeatedly. The resulting powders are then canned and hot-extruded to produce solid metal.

3.2 CHEMICAL STRUCTURE

An alloy can be created without melting, by violently deforming mixtures of different powders. The intense deformation associated with mechanical alloying can force atoms into positions where they may not prefer to be at equilibrium.

A solution which is homogeneous will nevertheless exhibit concentration differences of increasing magnitude as the size of the region which is chemically analysed decreases. These are random fluctuations which obey the laws of stochastic processes, and represent the real distribution of atoms in the solution. These equilibrium variations cannot usually be observed directly because of the lack of spatial resolution and noise in the usual microanalytical techniques. The fluctuations only become apparent when the resolution of chemical analysis falls to less than about a thousand atoms block.

Figure 3.2 illustrates the variation in the iron and chromium concentrations in fifty atom blocks, of the ferrite in a commercial alloy. There are real fluctuations but further analysis is needed to show whether they are beyond what is expected in homogeneous solutions

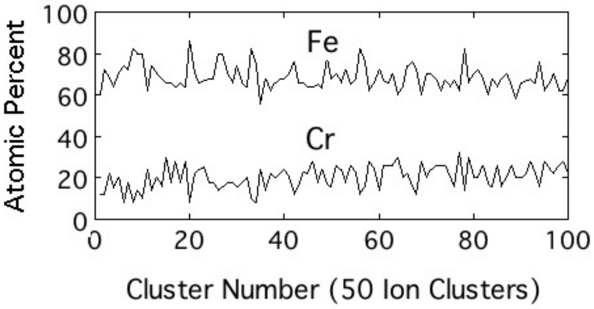

Figure 3.2 The variation in the iron and chromium concentrations of 50 atom samples of an alloy

For a random solution, the distribution of concentrations should be binomial since the fluctuations are random; any significant deviations from the binomial distribution would indicate either the clustering of lik–atoms or the ordering of unlike pairs.

The frequency distribution is obtained by plotting the total number of composition blocks with a given number of atoms of a specified element against the concentration. Figure 3.3 shows that the experimental distributions are essentially identical to the calculated binomial distributions, indicating that the solutions are random.

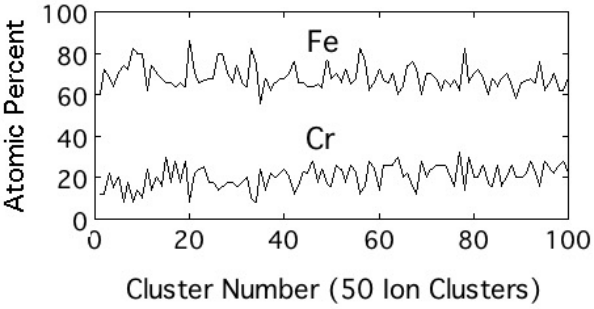

Figure 3.3 Frequency distribution curves for iron, chromium and aluminium in a mechanical alloy.

This does not mean that the solutions are thermodynamically ideal, but rather that the alloy preparation method which involves intense deformation forces a random dispersal of atoms. Indeed, Fe–Cr solutions are known to deviate significantly from ideality, with a tendency for like atoms to cluster. Thus, it can be concluded that the alloy is in a mechanically homogenised nonequilibrium state, and that prolonged annealing at low temperatures should lead to, for example, the clustering of chromium atoms.

3.3 SOLUTION FORMATION

The preparation of a binary alloy by this route can be considered in terms of the two elemental powders ('A' and 'B') which are mixed such that the mole fraction of B is x. The pure powders have the molar free energies μ_A° and μ_B° respectively, Figure 3.4. The free energy of this mechanical mixture of powders is given by:

$$G\{\text{mixture}\} = (1-x)\mu_A^\circ + x\mu_B^\circ + \Delta S_M \tag{3.1}$$

where ΔS_M is the accompanying change in configurational entropy. It has been assumed here, that there is no change in enthalpy in the process, i.e., the atoms in the context of bonding, are indifferent to the type of neighbouring atom.

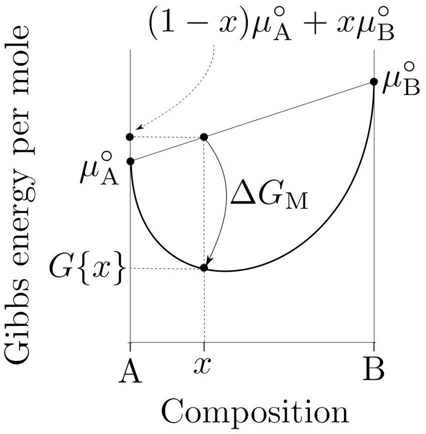

Figure 3.4 Plot of free energy versus composition, both for mechanical mixtures and a solid solution. ΔG_M is the free energy of mixing when the mechanical mixture turns into a solid solution.

The change in configurational entropy as a consequence of mixing can be obtained using the Boltzmann equation $S = k\ln\{w_c\}$ where w_c is the number of configurations. Suppose that there are m_A atoms per powder particle of A, and m_B atoms per particle of B; the powders are then mixed in a proportion which gives an average concentration of B which is the mole fraction x.

There is only one configuration when the heaps of powders are separate. When the powders are mixed randomly, the number of possible configurations for a mole of atoms becomes [96]:

$$\frac{\big(N_a([1-x]/m_A + x/m_B)\big)!}{(N_a[1-x]/m_A)!\ (N_a x/m_B)!}. \tag{3.2}$$

The numerator in equation 3.2 is the total number of particles and the denominator the product of the factorials of the A and B particles respectively; N_a is Avogadro's number. Using Stirling's approximation, the molar entropy of mixing is:

$$\begin{aligned}\frac{\Delta S_M}{kN_a} \quad = \quad & \frac{(1-x)m_B + xm_A}{m_A m_B}\ln\left\{N_a\frac{(1-x)m_B + xm_A}{m_A m_B}\right\}\\ & -\frac{1-x}{m_A}\ln\left\{\frac{N_a(1-x)}{m_A}\right\}\\ & -\frac{x}{m_B}\ln\left\{\frac{N_a x}{m_B}\right\}\end{aligned} \tag{3.3}$$

subject to the condition that the number of particles remains integral and non-zero.[1]

The largest reduction in free energy occurs when the particle sizes are atomic, Figure 3.5, which shows the molar free energy of mixing for a case where the average composition is equiatomic.

Such a composition maximises configurational entropy. When it is considered that phase changes often occur at appreciable rates when the accompanying reduction in free energy is just $10\,\mathrm{J\,mol^{-1}}$, Figure 3.5 shows that the entropy of mixing cannot be ignored when the particle size is less than a few hundreds of atoms. In commercial practice, powder metallurgically produced particles are typically 100 μm in size, in which case the entropy of mixing can be entirely neglected, though solution formation must be considered to be advanced when the processing reduces particle dimensions to some 10^2 atoms. These comments must be qualified due to the neglect any enthalpy change during mixing.

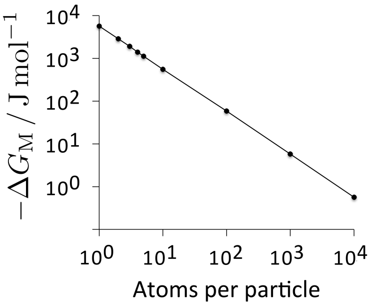

Figure 3.5 The molar Gibbs free energy of mixing, $\Delta G_\mathrm{M} = -T\Delta S_\mathrm{M}$, for a binary alloy, as a function of the particle size when all the particles are of uniform size in a mixture, the average composition of which is equiatomic. $T = 1000\,\mathrm{K}$.

3.4 ENTHALPY OF MIXING FOR PARTICULATE MIXTURES

The enthalpy of mixing will not in general be zero as was assumedabove. Equation 2.11 gives the molar enthalpy of mixing for atomic solutions. For particles which are not monatomic, only those atoms at the interface between the A and B particles will feel the influence of the unlike atoms. It follows that the enthalpy of mixing is not given by Equation 2.11, but rather by

$$\Delta H_\mathrm{M} = zN_a\omega 2\delta S_\mathrm{V}x(1-x)$$

where S_V is the amount of A-B interfacial area per unit volume and 2δ is the thickness of the interface, where δ represents a monolayer of atoms.

A further enthalpy contribution, which does not occur in conventional solution theory, is the structural component of the interfacial energy per unit area, σ:

$$\Delta HI = V_\mathrm{m}S_\mathrm{V}\sigma$$

where V_m is the molar volume.

Both of these equations contain the term V, which increases rapidly as the inverse of the particle size *m*. The model predicts that *solution formation is impossible* because the cost due to interfaces overwhelms any gain from binding energies or entropy. And yet, as demonstrated by atom-probe experiments, solutions do form during mechanical alloying, so there must be a mechanism to reduce interfacial energy as the particles are divided. The mechanism is the reverse of that associated with precipitation (Fig. **??**). A small precipitate can be coherent but the coherency strains become unsustainable as it grows. Similarly, during mechanical alloying it is conceivable that the particles must gain in coherence as their size diminishes. The milling process involves fracture and welding of the attrited particles so only those welds which lead to coherence might succeed.

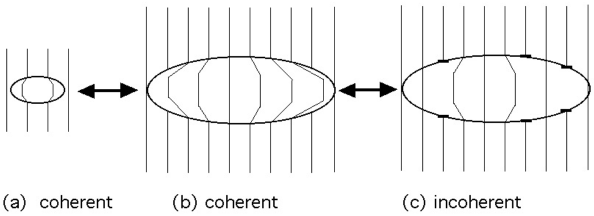

Figure 3.6 The change in coherence as a function of particle size. The lines represent lattice planes which are continuous at the matrix/precipitate interface during coherence, but sometimes terminate in dislocations for the incoherent state. Precipitation occurs in the sequence a→c whereas mechanical alloying is predicted to lead to a gain in coherence in the sequence c→a.

3.5 SHAPE OF FREE ENERGY CURVES

There are many textbooks which emphasise that free energy of mixing curves such as that illustrated in Fig. 2.2 must be drawn such that the slope is either $-\infty$ or $+\infty$ at $x = 0$ and $x = 1$ respectively. This is a straightforward result from equation 19 which shows that

$$\frac{\partial \Delta S_{\mathrm{M}}}{\partial x} = -kN_{\mathrm{a}} \ln\left\{\frac{x}{1-x}\right\}$$

so that the slope of $-T\Delta S_{\mathrm{M}}$ becomes $\pm\infty$ at the extremes of concentration. Notice that at those extremes, any contribution from the enthalpy of mixing will be finite and negligible by comparison, so that the free energy of mixing curve will also have slopes of $\pm\infty$ at the vertical axes corresponding to the pure components. Note that the intercepts at the vertical axes representing the pure components are nevertheless finite, with values μ_{A}^{0} and μ_{B}^{0}. It follows that the free energy of mixing of any solution from its components will at first decrease at an infinite rate.

However, these conclusions are strictly valid only when the concentration is treated as a *continuous* variable which can be as close to zero or unity as desired. The discussion here emphasises that there is a *discrete* structure to solutions. Thus, when considering N particles, the concentration can never be less than $1/N$ since the smallest amount of solute is just one particle. The slope of the free energy curve will not therefore be $\pm\infty$ at the pure components, but rather a finite number depending on the number of particles involved in the process of solution formation. Since the concentration is not a continuous variable, the free energy 'curve' is not a curve, but is better represented by a set of points representing the discrete values of concentration that are physically possible when mixing particles. Obviously, the shape approximates to a curve when the number of particles is large, as is the case for an atomic solution made of a mole of atoms. But the *curve* remains an approximation.

4 Computer calculation of phase diagrams

The thermodynamic methods described thus far in this chapter are revealing and have been applied towards the understanding and modelling the behaviour of iron and its alloys. It nevertheless is too complicated in the context of multicomponent steels where individual solute concentrations can vary over a large range. Therefore, methods have been developed for doing this in a seamless manner; these methods have been so successful that they now represent the first step in any alloy development project. The subject of the computer calculation of phase diagrams based on experimental data has been reviewed extensively, e.g., [124–129]. The focus here is on the framework for such generic calculations, which necessarily involves a degree of educated, clever empiricism. The process has also led to the systematic compilation and assessment of experimental data on a scale that is perhaps unique in science. All this was initiated by like-minded scientists long before "big data" or computer modelling became fashionable.

One possibility is to represent thermodynamic quantities by a series expansion with sufficient adjustable parameters to adequately fit the experimental data. There has to be a compromise between the accuracy of the fit and the number of terms in expansion. However, such expansions do not generalise well when dealing with complicated phase diagram calculations involving many components and phases. Experience suggests that the specific heat capacities for the pure elements are better represented by a polynomial with a form that describes most of the known experimental data:

$$C_{\mathrm{P}} = b_8 + b_9 T + b_{10} T^2 + \frac{b_{11}}{T^2}. \tag{4.1}$$

If the fit with experimental data is found not to be good enough, the polynomial is applied to a range over which the fit is satisfactory, and more than one polynomial is used to represent the full dataset with care exercised to ensure continuity over the range. A standard element reference state is defined with a list of the measured enthalpies and entropies of the pure elements at 298 K and one atmosphere pressure, for the crystal structure appropriate for these conditions. With respect to this state, the Gibbs free energy is obtained by integration to be:

$$G = b_{12} + b_{13} T + b_{14} T \ln\{T\} + b_{15} T^2 + b_{16} T^3 + \frac{b_{17}}{T}. \tag{4.2}$$

This free energy is defined with respect to a reference (included in b_{12}) i.e., relative to the enthalpy at 298.15 K and entropy at 0 K of the stable states of the element(s) concerned at 298.15 K. Allotropic transformations can be included if the transition temperatures, enthalpy of transformation and the C_{P} coefficients for all the phases are known.

Any specific contributions to C_{P}, such as due to magnetic transitions, are dealt with separately, as are the effects of pressure. Once again, the equations for these effects are chosen carefully in order to maintain generality.

The excess Gibbs free energy for a binary solution with components A and B is written:

$$\Delta_{\mathrm{e}} G_{\mathrm{AB}} = x_{\mathrm{A}} x_{\mathrm{B}} \sum_{i=0}^{j} L_{\mathrm{AB},i} (x_{\mathrm{A}} - x_{\mathrm{B}})^i. \tag{4.3}$$

For $i = 0$ this gives a term $x_{\mathrm{A}} x_{\mathrm{B}} L_{\mathrm{AB},0}$ which is familiar in regular solution theory, where the coefficient $L_{\mathrm{AB},0}$ is, as usual, independent of chemical composition and to a first approximation describes the interaction between components A and B. If all other $L_{\mathrm{AB},i}$ are zero for $i > 0$ then the equation reduces to the regular solution model with $L_{\mathrm{AB},0}$ as the regular solution parameter. Further terms $(i > 0)$ are added to allow for any composition dependence not described by the regular solution constant.

In the first approximation, the excess free energy of a ternary solution can be represented purely by a combination of the binary terms in Equation 4.3:

$$\begin{aligned}\Delta_{\mathrm{e}} G_{\mathrm{ABC}} &= x_{\mathrm{A}} x_{\mathrm{B}} \sum_{i=0}^{j} L_{\mathrm{AB},i}(x_{\mathrm{A}} - x_{\mathrm{B}})^i \\ &\quad + x_{\mathrm{B}} x_{\mathrm{C}} \sum_{i=0}^{j} L_{\mathrm{BC},i}(x_{\mathrm{B}} - x_{\mathrm{C}})^i + x_{\mathrm{C}} x_{\mathrm{A}} \sum_{i=0}^{j} L_{\mathrm{CA},i}(x_{\mathrm{C}} - x_{\mathrm{A}})^i.\end{aligned}$$

The advantage of the representation embodied in Equation 4.3 is clear, that for the ternary case, the relation reduces to the binary problem when one of the components is set to be identical to another, e.g., B≡C [130].

Experimental data may indicate significant ternary interactions, in which case a term $x_{\mathrm{A}} x_{\mathrm{B}} x_{\mathrm{C}} L_{\mathrm{ABC},0}$ is added to the excess free energy. If this does not adequately represent the deviation from the binary summation, then it can be converted into a series which properly reduces to a binary formulation when there are only two components:

$$\begin{aligned}x_{\mathrm{A}} x_{\mathrm{B}} x_{\mathrm{C}} \quad & \Big[L_{\mathrm{ABC},0} + \frac{1}{3}(1 + 2x_{\mathrm{A}} - x_{\mathrm{B}} - x_{\mathrm{C}}) L_{\mathrm{ABC},1} \\ & + \frac{1}{3}(1 + 2x_{\mathrm{B}} - x_{\mathrm{C}} - x_{\mathrm{A}}) L_{\mathrm{BCA},1} + \frac{1}{3}(1 + 2x_{\mathrm{C}} - x_{\mathrm{A}} - x_{\mathrm{B}}) L_{\mathrm{CAB},1}\Big].\end{aligned}$$

This method can be extended to any number of components as long as appropriate thermodynamic data are available, with the advantage that few coefficients have to be changed when the data due to one component are improved. The information necessary to derive the coefficients become sparse for systems with more than three components.

5 Thermodynamics of irreversible processes

Thermodynamics as a subject is limited to the equilibrium state. Properties such as entropy and free energy are, on an appropriate scale, static and time-invariant during equilibrium. There is an extension of the subject to systems that are close to equilibrium so that they can be divided into subsystems where the rules of equilibrium can be applied locally [139]. Parameters not relevant to the discussion of equilibrium, such as thermal conductivity, diffusivity and viscosity, then enter the picture because they can describe a second kind of time independence, that of the steady state. For example, the concentration profile does not change during steady-state diffusion, even though energy is being dissipated during diffusion.

The thermodynamics of irreversible processes deals with systems that are not at equilibrium but are nevertheless *stationary*. The theory in effect uses thermodynamics to deal with *kinetic* phenomena. There is nevertheless, a distinction between the thermodynamics of irreversible processes and kinetics. The former applies strictly to the steady-state, whereas there is no such restriction on kinetic theory.

5.1 REVERSIBILITY

A process, the direction of which can be changed by an infinitesimal alteration in the external conditions is called reversible, because an exact reversal leads to no net dissipation of energy. Figure 5.1 shows the response of an ideal gas contained at uniform pressure within a cylinder, any change being achieved by the motion of the piston. For any starting point on the pressure-volume curve, the application of an infinitesimal force may cause the piston to move to an adjacent position still on the curve, while the removal of the infinitesimal force restores the system to its original state. This process is reversible because there is no net dissipation in displacing and recovering the frictionless piston.

If the motion of the piston in the cylinder entails friction, then deviations occur from the P/V curve as illustrated by the cycle in Figure 5.1. An infinitesimal force cannot move the piston because energy must be dissipated to overcome the friction; this energy is the area enclosed by the cycle on the P/V plot. A process such as this, which involves the dissipation of energy, is classified as irreversible with respect to an infinitesimal change in the external conditions. More generally, reversibility means that it is possible to pass from one state to another without appreciable deviation from equilibrium. Real process are not reversible so equilibrium thermodynamics can only be used

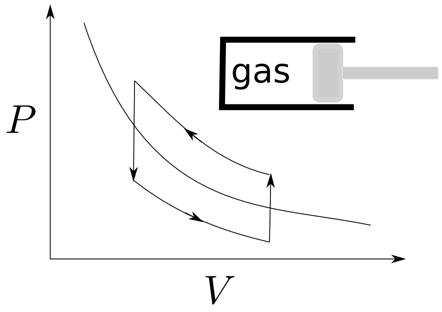

Figure 5.1 The curve represents the variation in pressure within the cylinder as the volume of the ideal gas is altered by the frictionless positioning the piston. The cycle represents the dissipation of energy when the motion of the piston causes friction.

approximately, though the same principles define whether or not a process can occur spontaneously without ambiguity.

For irreversible processes the *equations* of classical thermodynamics become *inequalities*. For example, at the equilibrium melting temperature, the free energies of the liquid and solid are identical ($G_{\text{liquid}} = G_{\text{solid}}$) but not so below that temperature ($G_{\text{liquid}} > G_{\text{solid}}$). Such inequalities are much more difficult to deal with though they indicate the natural direction of change. For steady-state processes however, the thermodynamic framework for irreversible processes as developed by Onsager [140] is particularly useful in obtaining relationships even though the system may not be at equilibrium.

5.1.1 LINEAR LAWS

There is no change in entropy or free energy at equilibrium. An irreversible process dissipates energy and entropy is created continuously. In the example illustrated in Fig. 5.1, the dissipation was due to friction; diffusion ahead of a moving interface is dissipative. The rate at which energy is dissipated is the product of the temperature and the rate of entropy production:

$$T\dot{S} = JX \tag{5.1}$$

where J is a generalised flux of some kind, and X a generalised force. In the case of an electrical current, the heat dissipation is the product of the current (J) and the electromotive force (X).

As long as the flux-force sets can be expressed as in Equation 5.1, the flux must naturally depend in some way on the force. It may then be written as a function $J\{X\}$ of the force X. At equilibrium, the force is zero. $J\{X\}$ can be expanded in a Taylor series about equilibrium ($X = 0$):

$$\begin{aligned} J\{X\} &= \sum_{0}^{\infty} a_n X^n \\ &= J\{0\} + J'\{0\}\frac{X}{1!} + J''\{0\}\frac{X^2}{2!}\ldots \end{aligned} \tag{5.2}$$

In this expansion, $J\{0\} = 0$ because there is no flux in the absence of force. If the high order terms are neglected then a proportionality between the force and flux is revealed:

$$J \propto X.$$

Therefore, the forces and their conjugate fluxes are linearly related whenever the dissipation can be expressed as in Equation 5.2, at least when the deviations from equilibrium are not large. This caveat is illustrated nicely by the relationship between the rate at which an interface moves and the driving force. In Chapter **??**, Equation **??**, which is limited to small driving forces, shows a linear relationship between the two quantities, whereas Equation **??** which is derived without limits on the magnitude of the driving force, shows that the rate and driving force are *not* in general linearly related.

In another example, consider a closed system in which a quantity dH of heat is transferred in a time interval dt across an area A in a direction z normal to that area, from a region at temperature T_{h} to a lower temperature T_ℓ. The receiving part increases its entropy by dH/T_ℓ whereas the depleted region experiences a reduction dH/T_{h}, so the change in entropy is

$$\mathrm{d}S = \mathrm{d}H\left(\frac{1}{T_\ell} - \frac{1}{T_{\text{h}}}\right).$$

The rate of entropy production per unit volume is therefore

$$\dot{S} = \frac{1}{V}\frac{\mathrm{d}S}{\mathrm{d}t} = \frac{1}{V}\frac{\mathrm{d}H}{\mathrm{d}t}\left(\frac{1}{T_\ell} - \frac{1}{T_{\text{h}}}\right). \tag{5.3}$$

The flux of heat J is defined as $A^{-1}\mathrm{d}H/\mathrm{d}t$ so Equation 5.3 becomes

$$\begin{aligned}\dot{S} &= J\frac{A}{V}\left(\frac{1}{T_\ell}-\frac{1}{T_\mathrm{h}}\right) \equiv J\left(-\frac{1}{T^2}\right)\frac{\mathrm{d}T}{\mathrm{d}z} \\ \text{or}\quad T\dot{S} &= \underbrace{J}_{\text{flux}}\underbrace{\left(-\frac{1}{T}\right)\frac{\mathrm{d}T}{\mathrm{d}z}}_{\text{force}}\end{aligned}$$

Some examples of forces and fluxes in their generic form are listed in Table 5.1.

Table 5.1

Examples of forces and their conjugate fluxes. z is the distance over which the gradient exists, ϕ is the electrical potential and μ the chemical potential.

Force	Flux
$-\frac{\partial\phi}{\partial z}$	Electrical Current
$-\frac{1}{T}\frac{\partial T}{\partial z}$	Heat flux
$-\frac{\partial\mu_i}{\partial z}$	Diffusion flux
Stress	Strain rate

5.1.2 MULTIPLE IRREVERSIBLE PROCESSES

There are circumstances whereby a number of irreversible processes occur together. In a ternary Fe-Mn-C alloy, the diffusion flux of carbon depends not only on the gradient of carbon, but also on that of manganese. A uniform distribution of carbon will tend to become inhomogeneous in the presence of a manganese concentration gradient. Similarly, the flux of heat may not depend on the temperature gradient alone; heat can be driven also by an electromotive force (Peltier effect).[1] Electromigration involves diffusion that is driven by an electromotive force. When there is more then one dissipative process, the total energy dissipation rate can still be written

$$T\dot{S} = \sum_i J_i X_i. \tag{5.4}$$

In general, if there is more than one irreversible process occurring, it is found *experimentally* that each flow J_i is related not only to its conjugate force X_i, but is also linearly related to all other forces present. Thus,

$$J_i = M_{ij}X_j \tag{5.5}$$

with $i,\ j = 1,2,3\ldots$. Therefore, a given flux depends on all the forces causing the dissipation of energy.

5.1.3 ONSAGER RECIPROCAL RELATIONS

Equilibrium in real systems is dynamic on a microscopic scale. It seems obvious that to maintain equilibrium under these dynamic conditions, a process and its reverse must occur at the same rate on the microscopic scale. The consequence is that provided the forces and fluxes are chosen from the dissipation equation and are independent, $M_{ij} = M_{ji}$. This is known as the Onsager theorem, or the

Onsager reciprocal relations. It applies to systems near equilibrium when the properties of interest have even parity, and assuming that the fluxes and their corresponding forces are independent. An exception occurs with magnetic fields in which case there is a sign difference $M_{ij} = -M_{ji}$ [141].

6 Quasichemical solution

The regular solution model assumes a random distribution of atoms even though the enthalpy of mixing is not zero. whereas in reality a random solution is only expected at high temperatures when the entropy term overwhelms any tendency for ordering or clustering of atoms. It follows that the configurational entropy of mixing should therefore vary with the temperature. The *quasichemical* solution model has a better treatment of configurational entropy which accounts for a non-random distribution of atoms. The model is so-called because it has a mass-action equation that has similarity to chemical reactions [100]. However, the presentation below follows derivations by Christian [101] and Lupis [97].

Recalling that zN_{AB} represents the number of A-B bonds, the total energy of the assembly for a particular value of N_{AB} is $U_{N_{\mathrm{AB}}} = -z(N_{\mathrm{A}}\varepsilon_{\mathrm{AA}} + N_{\mathrm{B}}\varepsilon_{\mathrm{BB}} - N_{\mathrm{AB}}\omega)$ where $\omega = \varepsilon_{\mathrm{AA}} + \varepsilon_{\mathrm{BB}} - 2\varepsilon_{\mathrm{AB}}$. In a non-random solution there are many values that N_{AB} can adopt; each value corresponding to one or more arrangement of atoms with an identical value of U is therefore associated with a degeneracy $g_{N_{\mathrm{AB}}}$ which is the number of arrangements possible for a given value of U. The partition function is therefore the sum over all possible N_{AB}:

$$\begin{aligned}\Omega &= \sum_{N_{\mathrm{AB}}} g_{N_{\mathrm{AB}}} \exp\left\{-\frac{U_{N_{\mathrm{AB}}}}{kT}\right\} \\ &= \sum_{N_{\mathrm{AB}}} g_{N_{\mathrm{AB}}} \exp\left\{\frac{z(N_{\mathrm{A}}\varepsilon_{\mathrm{AA}} + N_{\mathrm{B}}\varepsilon_{\mathrm{BB}} - N_{\mathrm{AB}})\omega}{kT}\right\}. \end{aligned} \tag{6.1}$$

For a given value of N_{AB}, the different non-interacting *pairs* of atoms can be arranged in the following number of ways $(N = N_{\mathrm{A}} + N_{\mathrm{B}})$

$$g_{N_{\mathrm{AB}}} \propto \frac{(\frac{1}{2}zN)!}{(\frac{1}{2}z[N_{\mathrm{A}} - N_{\mathrm{AB}}])!\,(\frac{1}{2}z[N_{\mathrm{B}} - N_{\mathrm{AB}}])!\,(\frac{1}{2}zN_{\mathrm{AB}})!\,(\frac{1}{2}zN_{BA})!} \tag{6.2}$$

where the first and second terms in the denominator refer to the numbers of A-A and B-B bonds respectively, and the third and fourth terms the numbers of A-B and B-A pairs respectively. This is not an equality because the various pairs are not independent, as illustrated in (Figure 6.1); the distribution of pairs is not random. Guggenheim addressed this difficulty by using a normalisation factor such that the summation of all possible degeneracies equals the total number of possible configurations as follows.

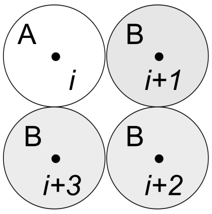

Figure 6.1 Why pairs of atoms cannot be distributed at random on lattice sites which are marked as small dots. Once the bonds connecting the coordinates $(i, i+1)$, $(i+1, i+2)$, $(i+2, i+3)$ are made as illustrated, the final bond connecting $(i, i+3)$ is necessarily occupied by a pair AB. Adapted from Lupis [97].

Suppose that the number of arrangements of pairs of atoms possible in a random solution is identified with an asterix, then from the proportionality 6.2, it is seen that

$$g^* \propto \frac{(\frac{1}{2}zN)!}{(\frac{1}{2}z[N_{\mathrm{A}} - N^*_{\mathrm{AB}}])!\,(\frac{1}{2}z[N_{\mathrm{B}} - N^*_{\mathrm{AB}}])!\,(\frac{1}{2}zN^*_{\mathrm{AB}})!\,(\frac{1}{2}zN^*_{BA})!}. \tag{6.3}$$

This again will overestimate the number of possibilities (Figure 6.1), but for a random solution it is known already that

$$g^* = \frac{N!}{N_\mathrm{A}!\,N_\mathrm{B}!}. \tag{6.4}$$

It follows that g_{N_AB} can be normalised as

$$g_{N_\mathrm{AB}} = \frac{(\frac{1}{2}z[N_\mathrm{A}-N^*_\mathrm{AB}])!\,(\frac{1}{2}z[N_\mathrm{B}-N^*_\mathrm{AB}])!\,(\frac{1}{2}zN^*_\mathrm{AB})!\,(\frac{1}{2}zN^*_{BA})!}{(\frac{1}{2}z[N_\mathrm{A}-N_\mathrm{AB}])!\,(\frac{1}{2}z[N_\mathrm{B}-N_\mathrm{AB}])!\,(\frac{1}{2}zN_\mathrm{AB})!\,(\frac{1}{2}zN_{BA})!} \times \frac{N!}{N_\mathrm{A}!\,N_\mathrm{B}!}. \tag{6.5}$$

With this, the partition function Ω is defined explicitly and the problem is in principle solved. It is usual however, to simplify first by assuming that the sum in Equation 6.1 can be replaced by its maximum value. This is because the thermodynamic properties that follow from the partition function depend on its logarithm, in which case the use of the maximum is a good approximation. The equilibrium number N^e_AB of A-B bonds may then be obtained by setting $\partial \ln\{\Omega\}/\partial N_\mathrm{AB} = 0$ [97, 101]:

$$N^\mathrm{e}_\mathrm{AB} = \frac{2Nzx(1-x)}{\beta_\mathrm{q}+1} \tag{6.6}$$

with β_q being the positive root of the equation

$$\beta_\mathrm{q}^2 - (1-2x) = 4x(1-x)\exp\{2\omega/kT\}, \tag{6.7}$$

so that

$$N^\mathrm{e}_\mathrm{AB} = \frac{2Nzx(1-x)}{[1-2x+4x(1-x)\exp\{2\omega/kT\}]^{\frac{1}{2}}+1}.$$

The percentages of the different pairs are plotted in Figure 6.2. Equation 6.6 obviously corresponds to the regular solution model if $\beta_\mathrm{q} = 1$ with a random arrangement of atoms. As expected, the number of unlike pairs is reduced when clustering is favoured, and increased when ordering is favoured.

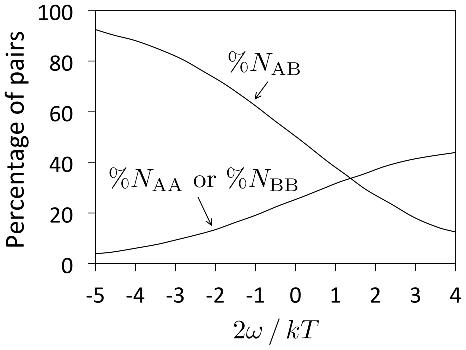

Figure 6.2 Calculated percentages of pairs for the quasichemical model with $x = (1-x) = 0.5$. The result is independent of the coordination number z.

The free energy of the assembly is

$$G = F = -kT\ln\{\Omega\} = U_{N^\mathrm{e}_\mathrm{AB}} - kT\ln g_{N^\mathrm{e}_\mathrm{AB}} \tag{6.8}$$

so that the free energy of mixing per mole becomes

$$\begin{aligned}\Delta G_\mathrm{M} &= zN^\mathrm{e}_\mathrm{AB}\,\omega - N_\mathrm{a}kT\ln g_{N^\mathrm{e}_\mathrm{AB}}\\ &= \underbrace{\frac{2z\omega N_\mathrm{a}x(1-x)}{\beta_\mathrm{q}+1}}_{\text{molar enthalpy of mixing}} - RT\ln g_{N^\mathrm{e}_\mathrm{AB}}.\end{aligned} \tag{6.9}$$

The second term on the right-hand side has the contribution from the configurational entropy of mixing. By substituting for $g_{N^{e}_{AB}}$, and with considerable manipulation, Christian has shown that this can be written in terms of β_q so that the molar free energy of mixing becomes:

$$\begin{aligned}\Delta G_M = & \frac{2z\omega N_a x(1-x)}{\beta_q+1} \\ & +RT\left[(1-x)\ln\{1-x\}+x\ln\{x\}\right] \\ & +\frac{1}{2}RTz\left\{(1-x)\ln\frac{\beta_q+1-2x}{(1-x)(\beta_q+1)}+x\ln\frac{\beta_q-1+2x}{x(\beta_q+1)}\right\}\end{aligned}$$

The second term in this equation is the usual contribution from the configurational entropy of mixing in a random solution, whereas the third term can be regarded as a quasichemical correction for the entropy of mixing because the atoms are not randomly distributed.

It is not possible to give explicit expressions for the chemical potential or activity coefficient since β_q is a function of concentration. Approximations using series expansions are possible [97] but the resulting equations are not as easy to interpret physically as the corresponding equations for the ideal or regular solution models.

The expressions in the quasichemical (or *first approximation*) clearly reduce to those of the regular solution (or *zeroth approximation*) model when $\beta_q = 1$. Although a better model has been obtained, the first approximation relies on the absence of interference between atom-pairs. However, each atom in a pair belongs to several pairs so that better approximations can be obtained by considering larger clusters of atoms in the calculation. Such calculations are known as the "cluster variation" method proposed originally by Kikuchi [102]. The improvements obtained with these higher approximations are usually rather small though there are cases where pairwise interactions simply will not do.

It is worth emphasising that although the quasichemical model has an excess entropy, this comes as a correction to the configurational entropy. The excess entropy from this model is always negative; as Lupis pointed out [97], there is more disorder in a random solution than in one that is biased. Therefore, the configurational entropy from the quasichemical model is always less than expected from an ideal solution. Thermal entropy or other terms such as magnetic or electronic are additional contributions.

The procedure in the development of the quasichemical models is illustrated in Figure 6.3.

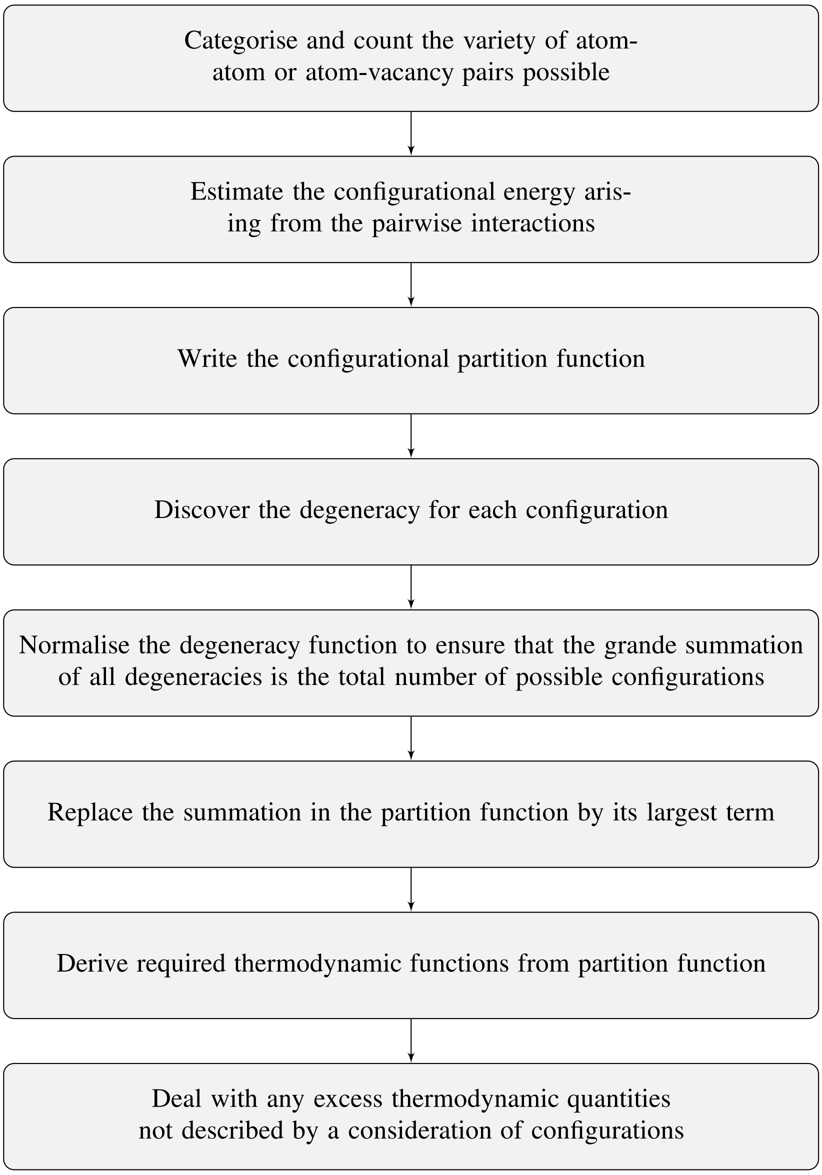

Figure 6.3 Steps in the construction of a quasichemical solution model.

REFERENCES

1. A. B. Pippard: Classical Thermodynamics: Cambridge, U. K.: Cambridge University Press, 1981.
2. C. Zener: ‘Kinetics of the decomposition of austenite’, *Trans. Am. Inst. Min. Metall. Engng.*, 1946, **167**, 550–595.
3. C. Zener: ‘Equilibrium relations in medium alloy steels’, *Trans. A.I.M.E.*, 1946, **167**, 513–534.
4. W. J. Moore: Physical Chemistry: 5th ed., New Jersey, USA: Prentice-Hall, 1972.
5. K. G. Denbigh: The principles of chemical equilibrium: 4th ed., Cambridge, U. K.: Cambridge University Press, 2018.
6. P. Debye: ‘Zur theorie der spezifischen wärmen’, *Annalen der Physik*, 1912, **344**, 789–839.

7. L. Kaufman, S. V. Radcliffe, and M. Cohen: ‘Thermodynamics of the bainite reaction’, In: V. F. Zackay, and H. I. Aaronson, eds. *Decomposition of Austenite by Diffusional Processes*. New York, USA: Interscience, 1962:313–352.
8. F. A. Lindemann: ‘Ueber die berechnung molekularer eigenfrequenzen (the calculation of molecular Eigen-frequencies)’, *Physikalische Zeitschrift*, 1910, **11**, 609–612.
9. L. Kaufman: ‘Estimation of the entropy of NaCl type compounds’, *Trans. Metall. Soc. AIME*, 1962, **224**, 1006–1009.
10. L. Kaufman, E. V. Clougherty, and R. J. Weiss: ‘The lattice stability of metals – iii iron’, *Acta Metallurgica*, 1963, **11**, 323–335.
11. L. D. Blackburn, L. Kaufman, and M. Cohen: ‘Phase transformations in iron-ruthenium alloys under high pressure’, *Acta Metallurgica*, 1965, **13**, 533–541.
12. F. H. Herbstein, and J. Smuts: ‘Determination of the Debye temperature of alpha-iron by X-ray diffraction’, *Philosophical Magazine*, 1963, **8**, 367–385.
13. G. L. Stepakoff, and L. Kaufman: ‘Thermodynamic properties of hcp iron and iron-ruthenium alloys’, *Acta Metallurgica*, 1968, **16**, 13–22.
14. R. L. Clendenen, and H. G. Drickamer: ‘The effect of pressure on the volume and lattice parameters of ruthenium an iron’, *Journal of the Physics and Chemistry of Solids*, 1964, **25**, 865–868.
15. H.-K. Mao, W. A. Bassett, and T. Takahashi: ‘Effect of pressure on crystal structure and lattice parameters of iron up to 300 kbar’, *Journal of Applied Physics*, 1967, **38**, 272–276.
16. A. H. Wilson: The theory of metals: Cambridge, U. K.: Cambridge University Press, 1958.
17. W. H. Keesom, and B. Kurrelmeyer: ‘The atomic heat of iron from 1.1° to 20.4°K’, *Physica*, 1939, **6**, 633–672.
18. J. A. Hofmann, A. Paskin, K. J. Tauer, and R. J. Weiss: ‘Analysis of ferromagnetic and antiferro-magnetic second-order transitions’, *Journal of Physics and Chemistry of Solids*, 1956, **1**, 45–60.
19. P. Wilkes: Solid state theory in metallurgy: Cambridge, U. K.: Cambridge University Press, 1973.
20. J. M. Ziman: Models of disorder: Cambridge, U. K.: Cambridge University Press, 1979.
21. I. M. K. Billas, A. Chatelain, and W. A. de Heer: ‘Magnetism from the atom to the bulk in iron, cobalt, and nickel clusters’, *Science*, 1994, **265**, 1682–1684.
22. A. J. Freeman, and R. Q. Wu: ‘Electronic structure theory of surface, interface and thin film magnetism’, *Journal of Magnetism and Magnetic Materials*, 1991, **100**, 497–514.
23. I. M. K. Billas, J. A. Baker, A. Chatelain, and W. A. de Heer: ‘Magnetic moments of iron clusters with 25 to 700 atoms and their dependence on temperature’, *Physical Review Letters*, 1993, **71**, 4067–4070.
24. L. C. nd X. L. Wan, and K. M. Wu: ‘Three-dimensional analysis of ferrite allotrimorphs nucleated on grain boundary faces, edges and corners’, *Materials Characterization*, 2010, **61**, 580–583.
25. L. Patrick: ‘The change in ferromagnetic Curie points with hydrostatic pressure’, *Physical Review*, 1954, **93**, 384–392.
26. J. A. Hoffmann, A. Paskin, K. J. Tauer, and R. J. Weiss: ‘Analysis of ferromagnetic and antiferromagnetic second-order transitions’, *Journal of the Physics and Chemistry of Solids*, 1956, **1**, 45–60.
27. C. Kittel: Introduction to Solid State Physics: 4th ed., New York, USA: John Wiley and Sons Inc., 1971.
28. L. Kaufman: ‘Condensed-state reactions at high pressures’, In: W. M. Mueller, ed. *Energetics in Metallurgical Phenomena*, vol. 3. New York, USA: Gordon and Breach Publishers, 1967:55–84.
29. D. C. Wallace, P. H. Sidles, and G. C. Danielson: ‘Specific heat of high purity iron by a pulse

heating method', *Journal of Applied Physics*, 1960, **31**, 168–176.

30. R. J. Weiss, and K. J. Tauer: 'Components of the thermodynamic functions of iron', *Physical Review*, 1956, **102**, 1490–1495.
31. H. A. Gersch, C. G. Shull, and M. K. Wilkinson: 'Critical magnetic scattering of neutrons by iron', *Physical Review*, 1956, **103**, 525–534.
32. G. Inden: 'Determination of chemical and magnetic interchange energies in bcc alloys', *Zeitschrift für Metallkunde*, 1975, **66**, 577–582.
33. M. Hillert, and M. Jarl: 'A model for alloying effects in ferromagnetic metals', *CALPHAD*, 1978, **2**, 227–238.
34. A. P. Miodownik: 'The calculation of magnetic contributions to phase stability', *C*, 1977, **1**, 133–158.
35. H. Ino, K. Hayashi, T. Otsuka, D. Isobe, K. Tokumitsu, and K. Oda: 'Appearance of ferromagnetism in fcc solid solutions of binary and ternary Fe-Cu based systems prepared by mechanical alloying techniques', *Materials Science & Engineering A*, 2001, **304-306**, 972–974.
36. H. H. Ettwig, and W. Pepperhoff: 'On magnetism of gamma-Fe-Ni-Mn alloys', *Physica Status Solidi A*, 1974, **23**, 105–111.
37. J. M. D. Coey: 'Magnetic localization and magnetoresistance in mixed-valence manganites and related ferromagnetic oxides', *Philosophical Transactions of the Royal Society A*, 1998, **356**, 1519–1541.
38. T. G. Perring, G. Aeppli, S. M. Hayden, Y. Tokura, Y. Moritomo, J. P. Remeika, and S.-W. Cheong: 'Magnetic dynamics in colossal magnetoresistive perovskite manganites', *Philosophical Transactions of the Royal Society, London*, 1998, **356**, 1563–1575.
39. K. J. Tauer, and R. J. Weiss: 'Unusual magnetic structure of face centered cubic Fe', *Bulletin of the American Physical Society*, 1961, **6**, 125.
40. R. J. Weiss, and A. S. Marotta: 'Spin-dependence of the resistivity of magnetic metals', *Journal of the Physics and Chemistry of Solids*, 1956, **9**, 302–308.
41. S. C. Abrahams, L. Guttman, and J. S. Kasper: 'Neutron diffraction determination of antiferromagnetism in face-centered cubic (gamma) iron', *Physical Reviews*, 1962, **127**, 2052–2055.
42. U. Gonser, C. J. Meechan, A. H. Muir, and H. Wiedersich: 'Determination of the néel temperatures in fcc iron', *Journal of Applied Physics*, 1963, **34**, 2373–2378.
43. R. J. Weiss: 'The origin of the 'Invar effect', *Proceedings of the Physics Society*, 1963, **82**, 281–288.
44. J. G. Wright: 'Ferromagnetism in epitaxial FCC iron films', *Philosophical Magazine*, 1971, **24**, 217–233.
45. U. Gonser, K. Irischel, and S. Nasu: 'Ferromagnetic ordering in fcc gamma-iron precipitates in Cu-Au alloys', *Journal of Magnetism and Magnetic Materials*, 1980, **15-18**, 1145–1146.
46. S. D. Bader, and E. R. Moog: 'Magnetic properties of novel epitaxial films', *Journal of Applied Physics*, 1987, **61**, 3729–3734.
47. J. Z. Jiang, and F. T. Chen: 'A study of the microstructure of mechanically alloyed fcc FeCu', *Journal of Physics – Condensed Matter*, 1994, **6**, L343–L348.
48. J. Z. Jiang, Q. A. Pankhurst, C. E. Johnson, C. Gente, and R. Borman: 'Magnetic properties of mechanically alloyed FeCu', *Journal of Physics – Condensed Matter*, 1994, **6**, L227–L232.
49. J. Z. Jiang, C. Gente, and R. Bormann: 'Mechanical alloying in the Fe-Cu system', *Materials Science & Engineering A*, 1998, **242**, 268–277.
50. K. J. Tauer, and R. J. Weiss: 'Magnetic second-order transitions', *Physical Reviews*, 1955, **100**, 1223–1224.
51. J. Kübler: 'Magnetic moments of ferromagnetic and antiferromagnetic bcc and fcc iron', *Physics Letters A*, 1981, **81**, 81–83.
52. G. L. Krasko: 'Metamagnetic behaviour of fcc iron', *Physical Review B*, 1987, **36**, 8565–8569.

53. P. Mohn, K. Schwarz, and D. Wagner: ‘Magnetoelastic anomalies in Fe-Ni invar alloys’, *Physical Review B*, 1991, **43**, 3318–3324.
54. E. F. Wassermann: ‘The invar problem’, *Journal of Magnetism and Magnetic Materials*, 1991, **100**, 346–362.
55. M. Nicol, and G. Jura: ‘Mössbauer spectrum of iron-57 in iron metal at very high pressure’, *Science*, 1963, **141**, 1035–1038.
56. D. N. Pipkorn, C. K. Edge, P. Debrunner, G. De Pasquali, H. G. Drickamer, and H. Frauenfelder: ‘Mössbauer effect in iron under very high pressure’, *Physical Review A*, 1964, **135**, 1604–1612.
57. J. S. Kouvel: ‘Magnetic properties of solids under pressure’, In: W. Paul, and D. M. Warschauer, eds. *Solids under pressure*. New York, USA: McGraw Hill, 1963:277–301.
58. K. Shimizu, T. Kimura, S. Furomoto, K. Takeda, K. Kontani, Y. Onuki, and K. Amaya: ‘Superconductivity in the non-magnetic state of iron under pressure’, *Nature*, 2001, **412**, 316–318.
59. V. Thakor, J. B. Staunton, J. Poulter, S. Ostanin, B. Ginatempo, and E. Bruno: ‘Ab initio calculations of incommensurate antiferromagnetic spin fluctuations in hcp iron under pressure’, *Physical Review B*, 2003, **67**, 180405.
60. S. Fox, and H. J. F. Jansen: ‘Structure and properties of trigonal iron’, *Physical Review B*, 1996, **53**, 5119–5122.
61. S. Peng, and H. J. F. Jansen: ‘Electronic structure of face-centered tetragonal iron’, *Journal of Applied Physics*, 1990, **67**, 4567–4569.
62. E. C. Bain: ‘The nature of martensite’, *Trans. AIME*, 1924, **70**, 25–46.
63. C. M. Wayman: ‘The growth of martensite since E C Bain (1924) - some milestones’, *Materials Forum*, 1990, **56-58**, 1–32.
64. S. S. Peng, and H. J. F. Jansen: ‘Structural and magnetic properties of tetragonally distorted iron’, *Ultramicroscopy*, 1992, **47**, 361–366.
65. B. T. Jonker, K. H. Walker, E. Kisker, G. A. Prinz, and C. Carbone: ‘Spin-polarized photoemission study of epitaxial Fe(001) films on Ag(001)’, *Physical Review Letters*, 1986, **57**, 142–143.
66. G. L. Krasko, and G. B. Olson: ‘Ferromagnetism and crystal lattice stability of bcc and fcc iron’, *Journal of Applied Physics*, 1990, **67**, 4570–4572.
67. H. C. Herper, E. Hoffmann, and P. Entel: ‘Ab initio investigations of iron-based martensitic stystems’, *Le Journal de Physique IV*, 1997, **7**, C5–71 – C5–76.
68. H. C. Herper, E. Hoffmann, and P. Entel: ‘Ab initio full-potential study of the structural and magnetic phase stability of iron’, *Physical Review B*, 1999, **60**, 3839–3848.
69. C. Li, A. J. Freeman, H. J. F. Jansen, and C. L. Fu: ‘Magnetic anisotropy in low-dimensional ferromagnetic systems: Fe monolayers on Ag (001), Au(001) and Pd(001) substrates’, *Physical Review B*, 1990, **42**, 5433–5422.
70. H. J. Haugan, B. D. McCombe, and P. G. Mattocks: ‘Structural and magnetic properties of thin epitaxial Fe films on (110) GaAs prepared by metalorganic chemical vapor deposition’, *Journal of Magnetism and Magnetic Materials*, 2002, **247**, 296–304.
71. A. S. Edelstein, J. S. Murday, and B. B. Rath: ‘Challenges in nanomaterials design’, *Progress in Materials Science*, 1997, **42**, 5–21.
72. J. H. van Vleck: ‘On the anisotropy of cubic ferromagnetic crystals’, *Physical Review*, 1937, **52**, 1178–1198.
73. C. Stamm, F. Marty, A. Vaterlaus, V. Weich, S. Egger, U. Maier, U. Ramsperger, H. Fuhrmann, and D. Pescia: ‘Two-dimensional magnetic particles’, *Science*, 1998, **282**, 449–451.
74. S. T. Purcell, B. Heinrich, and A. S. Arrott: ‘Perpendicular anisotropy at the (001) surface of bulk iron single crystals’, *Journal of Applied Physics*, 1988, **64**, 5337–5339.
75. R. F. Willis, J. A. C. Bland, and W. Schwarzacher: ‘Ferromagnetism in ultrathin metastable films of fcc Fe, Co, Ni’, *Journal of Applied Physics*, 1988, **63**, 4051–4056.

76. S. D. Bader, E. R. Moog, and P. Grunberg: 'Magnetic hysteresis of epitaxially deposited iron in the monolayer range: a Kerr effect experiment in surface magnetism', *Journal of Magnetism and Magnetic Materials*, 1986, **53**, L295–L298.
77. T. Baykara, R. H. Hauge, N. Norem, P. Lee, and J. L. Margrave: 'A review of containerless thermophysical property measurements for liquid metals and alloys', *High Temperature and Materials Science*, 1994, **32**, 113–154.
78. R. I. L. Guthrie, and T. Iida: 'Thermodynamic properties of liquid metals', *Materials Science & Engineering A*, 1994, **178**, 35–41.
79. R. I. Orr, and J. Chipman: 'Thermodynamic functions of iron', *TMS-AIME*, 1967, **239**, 630–633.
80. W. W. Anderson, and T. J. Ahrens: 'An equation of state for liquid iron and implications for the Earth's core', *Journal of Geophysical Research*, 1994, **99**, 4273–4284.
81. L. Kaufman: 'Thermodynamics of martensitic fcc$\rightleftharpoons$bcc and fcc$\rightleftharpoons$hcp transformations in the iron-ruthenium system', In: *Physical properties of martensite and bainite, Special Report 93*. London, U.K.: Iron and Steel Institute, 1965:49–52.
82. G. P. Tiwari: 'Modification of Richard's rule and correlation between entropy of fusion and allotropic behaviour', *Metal Science*, 1978, **12**, 317–320.
83. J. Mo, H. Liu, Y. Zhang, M. Wang, L. Zhang, B. Liu, and W. Yang: 'Effects of pressure on structure and mechanical property in monatomic metallic glass', *Journal of Non-Crystalline Solids*, 2017, **464**, 1–4.
84. C. V. Thompson, and F. Spaepen: 'On the approximation of the free energy change on crystallisation', *Acta Metallurgica*, 1979, **27**, 1855–1859.
85. J. D. Hoffman: 'Thermodynamic driving force in nucleation and growth processes', *Journal of Chemical Physics*, 1958, **29**, 1192–1193.
86. D. R. H. Jones, and G. A. Chadwick: 'An expression for the free energy of fusion in the homogeneous nucleation of solid from pure melts', *Philosophical Magazine*, 1971, **190**, 995–998.
87. L.-G. Liu, and W. A. Bassett: 'The melting of iron up to 200 kbar', *Journal of Geophysical Research*, 1975, **80**, 3777–3782.
88. J. H. Nguyen, and N. C. Holmes: 'Melting of iron at the physical conditions of the Earth's core', *Nature*, 2004, **427**, 339–342.
89. O. L. Anderson, and D. G. Isaak: 'Another look at the core density deficit of earth's outer core', *Physics of the Earth and Planetary Interiors*, 2002, **131**, 19–27.
90. H. Ichikawa, T. Tsuchiya, and Y. Tange: 'The P-V-T equation of state and thermodynamic properties of liquid iron', *Journal of Geophysical Research*, 2014, **119**, 240–252.
91. D. Gerlich, and S. Hart: 'Pressure dependence of the elastic moduli of three austenitic stainless steels', *Journal of Applied Physics*, 1984, **55**, 880–884.
92. M. Müller, P. Erhart, and A. Karsten: 'Analytic bond-order potential for bcc and fcc iron—comparison with established embedded-atom method potentials', *Journal of Physics – Condensed Matter*, 2007, **19**, 3262220.
93. H. K. Mao, Y. Wu, L. C. Chen, and J. F. Shu: 'Static compression of iron to 300 GPa and $Fe_{0.8}Ni_{0.2}$ alloy to 260 GPa: implications for composition of the core', *Journal of Geophysical Research*, 1990, **95**, 21737–21742.
94. M. W. Guinan, and D. N. Beshers: 'Pressure derivatives of the elastic constants of α-iron to 10 kb', *Journal of the Physics and Chemistry of Solids*, 1968, **29**, 541–549.
95. J. S. Benjamin: 'oxide dispersion strengthened ods superalloys directional recrystallisation', *Metallurgical Transactions*, 1970, **1**, 2943–2951.
96. A. Y. Badmos, and H. K. D. H. Bhadeshia: 'Evolution of solutions', *Metallurgical & Materials Transactions A*, 2000, **28**, 2189–2193.
97. C. H. P. Lupis: Chemical thermodynamics of materials: New York, USA: North-Holland,

1983.

98. J. H. Hildebrand: 'Solubility. xii. regular solutions', *Journal of the American Chemical Society*, 1929, **51**, 66–80.
99. E. A. Guggenheim: 'The statistical mechanics of regular solutions', *Proceedings fo the Royal Society A*, 1935, **148**, 304–312.
100. E. A. Guggenheim: Mixtures: Oxford, U. K.: Oxford University Press, 1952.
101. J. W. Christian: Theory of Transformations in Metals and Alloys, Part I: 2 ed., Oxford, U. K.: Pergamon Press, 1975.
102. R. Kikuchi: 'A theory of cooperative phenomena', *Physical Review*, 1951, **81**, 988–1003.
103. R. B. McLellan, and W. W. Dunn: 'A quasichemical treatment of interstitial solid solutions: its application to carbon in austenite', *Journal of Physics and Chemistry of Solids*, 1969, **30**, 2631–2637.
104. W. W. Dunn, and R. B. McLellan: 'The application of a quasichemical solid solution model to carbon in austenite', *Metallurgical Transactions*, 1970, **1**, 1263–1265.
105. S. Ban-Ya, J. F. Elliott, and J. Chipman: 'Activity of C in Fe-C alloys at 1150 C', *Trans. Metall. Soc. AIME*, 1969, **245**, 1199–1206.
106. S. Ban-Ya, J. F. Elliott, and J. Chipman: 'Thermodynamics of austenitic Fe-C alloys', *Metallurgical Transactions*, 1970, **1**, 1313–1320.
107. K. Alex, and R. B. McLellan: 'A zeroth order mixing treatment of interstitial solid solutions', *Journal of the Physics and Chemistry of Solids*, 1970, **31**, 2751–2753.
108. H. K. D. H. Bhadeshia: 'Quasichemical model for interstitial solutions', *Materials Science and Technology*, 1998, **14**, 273–276.
109. W. W. Dunn, and R. B. McLellan: 'The thermodynamic properties of carbon in body-centered cubic iron', *Metallurgical Transactions*, 1971, **2**, 1079–1086.
110. R. B. McLellan: 'The thermodynamics of dilute interstitial solid solutions', In: P. S. Rudman, and J. Stringer, eds. *Phase Stability in Metals and Alloys*. New York, USA: McGraw Hill, 1967:393–417.
111. L. Kaufman, and H. Nesor: 'Coupled phase diagrams and thermochemical data for transition metal binary systems - IV', *CALPHAD*, 1978, **2**, 295–318.
112. K. Oda, H. Fujimura, and H. Ino: 'Local interactions in carbon-carbon and carbon-M (M: Al, Mn, Ni) atomic pairs in fcc gamma-iron', *Journal of Physics – Condensed Matter*, 1994, **6**, 679–692.
113. A. L. Sozinov, A. G. Balanyuk, and V. G. Gavriljuk: 'C-C interaction in iron-base austenite and interpretation of Mössbauer spectra', *Acta Materialia*, 1997, **45**, 225–232.
114. V. M. Nadutov, L. A. Bulvain, and V. M. Garamus: 'Analysis of small-angle neutron scattering from Fe–18Cr–10Mn–16Ni–0.5N and Fe–21Cr–10Mn–17Ni–0.5C austenites', *Materials Science & Engineering A*, 1999, **264**, 286–290.
115. H. K. D. H. Bhadeshia: 'Application of first-order quasichemical theory to transformations in steels', *Metal Science*, 1982, **16**, 167–169.
116. Y. Mou, and H. I. Aaronson: 'The carbon carbon interaction energy in alpha Fe-C alloys', *Acta Metallurgica*, 1989, **37**, 757–765.
117. J. C. Fisher, J. H. Hollomon, and D. Turnbull: 'Kinetics of the austenite to martensite transformation', *Metals Transactions*, 1949, **185**, 691–700.
118. J. H. Jang, H. K. D. H. Bhadeshia, and D. W. Suh: 'Solubility of carbon in tetragonal ferrite in equilibrium with austenite', *Scripta Materialia*, 2012, **68**, 195–198.
119. A. G. Khachaturyan, and G. A. Shatalov: 'Elsatic-interaction potential of defects in a crystal', *Soviet Physics - Solid State*, 1969, **11**, 118–123.
120. A. G. Khachaturyan, and G. A. Shatalov: 'Theory of ordering of carbon-atoms in a martensite crystal', *Physics of Metals and Metallography*, 1971, **32**, 5–13.
121. A. G. Khachaturyan: Theory of phase transformations and structure of solid solutions: New

York, USA: John Wiley & Sons, Inc., 1983.

122. D. A. Mirzayev, A. Mirzoev, and P. V. Chirkov: ‘Ordering of carbon atoms in free martensite crystal and when enclosed in elastic matrix’, *Metallurgical & Materials Transactions A*, 2016, **47**, 637–640.
123. P. V. Chirkov, A. A. Mirzoev, and D. A. Mirzaev: ‘Role of stresses and temperature in the Z ordering of carbon atoms in the martensite lattice’, *Physics of Metals and Metallography*, 2016, **117**, 1138–1143.
124. L. Kaufman: ‘The stability of metallic phases’, *Progress in Materials Science*, 1969, **14**, 57–96.
125. T. G. Chart, J. F. Counsell, G. P. Jones, W. Slough, and P. J. Spencer: ‘Provision and use of thermodynamic data for the solution of high-temperature practical problems’, *International Metals Reviews*, 1975, **20**, 57–82.
126. M. Hillert: ‘Prediction of iron base phase diagrams’, In: D. V. Doane, and J. S. Krikaldy, eds. *Hardenability concepts with applications to steels*. Warrendale, Pennsylvania, USA: The Metallurgical Society of AIME, 1977:5–27.
127. I. Ansara: ‘Comparison of methods for the thermodynamica calculation of phase diagrams’, *International Metals Reviews*, 1979, **1**, 20–53.
128. G. Inden: ‘The role of magnetism in the calculation of phase diagrams’, *Physica B*, 1981, **103**, 82–100.
129. K. Hack, ed.: The SGTE Casebook: Thermodynamics at work: The Institute of Materials, London, 1996.
130. M. Hillert: ‘Empirical methods of predicting and representing thermodynamic properties of ternary solution phases’: Tech. Rep. 0143, Royal Institute of Technology, Stockholm, Sweden, 1979.
131. M. Hillert, and L. I. Staffansson: ‘The regular solution model for stoichiometric phases and ionic melt’, *Acta Chimica Scandinavica*, 1970, **24**, 3616–3626.
132. M. Temkin: ‘Mixtures of fused salts as ionic solutions’, *Acta Phsicochimica URSS*, 1945, **20**, 411–417.
133. M. H. M. Waldenström: ‘A thermodynamic analysis of the Fe-Mn-C system’, *Metallurgical & Materials Transactions A*, 1977, **8**, 5–13.
134. B. Uhrenius, and H. Harvig: ‘A thermodynamic evaluation of carbide solubilities in the Fe-Mo-C, Fe-W-C, and Fe-Mo-W-C systems at 1000 C’, *Metal Science*, 1975, **9**, 67–82.
135. B. Sundman, and J. Ågren: ‘A regular solution model for phases with several components and sublattices, suitable for computer applications’, *Journal of the Physics and Chemistry of Solids*, 1981, **42**, 297–301.
136. L. F. Bates: Modern Magnetism: Cambridge, U. K.: Cambridge University Press, 1963.
137. M. V. Nevitt, and A. T. Aldred: ‘Ferromagnetism in V-Fe and Cr-Fe alloys’, *Journal of Applied Physics*, 1963, **34**, 463–468.
138. G. Inden, and W. O. Meyer: ‘Approximate determination of the Curie temperatures of bcc Fe-Co alloys’, *Zietschrift für Metallkunde*, 1975, **66**, 725–727.
139. K. G. Denbigh: The thermodynamics of the steady state: New York, USA: John Wiley & Sons, Inc., 1955.
140. L. Onsager: ‘Reciprocal relations in irreversible processes – i’, *Physical Review*, 1931, **37**, 405–426.
141. D. G. Miller: ‘Thermodynamics of irreversible processes: The experimental verification of the Onsager reciprocal relations.’, *Chemical Reviews*, 1960, **60**, 15–37.
142. J. Z. Jiang, U. Gonser, C. Gente, and R. Bormann: ‘Mössbauer investigations of mechnical alloying in the Fe-Cu system’, *Applied Physics Letters*, 1993, **63**, 2768–2770.
143. J. Z. Jiang, U. Gonser, C. Gente, and R. Bormann: ‘Thermal stability of the unstable fcc-FeCu phase prepared by mechanical alloysing’, *Applied Physics Letters*, 1993, **63**, 1056–1058.

144. J. G. Gay, and R. Richter: ‘Spin anisotropy of ferromagnetic films’, *Physical Review Letters*, 1986, **56**, 2728–2731.
145. J. G. Gay, and R. Richter: ‘Spin anisotropy of ferromagnetic slabs and overlayers’, *Journal of Applied Physics*, 1987, **61**, 3362–3365.
146. J. H. Perepezko, and J. S. Paik: ‘Thermodynamic properties of undercooled liquid metals’, *Journal of non-crystalline solids*, 1984, **61**, 113–118.
147. G. J. Shiflet, J. R. Bradley, and H. I. Aaronson: ‘A re-examination of the thermodynamics of the proeutectoid ferrite transformation in steels’, *TMS-AIME*, 1978, **9A**, 999–1008.
148. A. H. Cottrell: ‘Constitutional vacancies in NiAl’, *Intermetallics*, 1995, **3**, 341–345.

Notes

[1] Hildebrand’s definition: “A regular solution is one involving no entropy change when a small amount of one of its components is transferred to it from an ideal solution of the same composition, the total volume remaining unchanged” [98].

[1] This equation reduces to the familiar

$$\Delta S_{\mathrm{M}} = -kN_{\mathrm{a}}[(1-x)\ln\{1-x\} + x\ln\{x\}] \tag{6.10}$$

when $m_{\mathrm{A}} = m_{\mathrm{B}} = 1$.

[1] In the Peltier effect, the two junctions of a thermocouple are kept at the same temperature but the passage of an electrical current causes one of the junctions to absorb heat and the other to liberate the same quantity of heat. This Peltier heat is found to be proportional to the current.